Mechatronics in Fuel Cell Systems

Anna G. Stefanopoulou[†]

[†]Mechanical Engineering Department, Univ of Michigan, Ann Arbor

Abstract: Power generation from Fuel Cells (FC) requires the integration of chemical, fluid, mechanical, thermal, electrical, and electronic subsystems. This integration presents many challenges and opportunities in the mechatronics field. In this paper we highlight important design issues and pose problems that require mechatronics solutions. We start by presenting the design process of a toy school bus powered by hydrogen. The FC toy bus was designed during an undergraduate student project. It was an effective and rewarding educational activity that revealed complex systems issues and familiarized us with the FC technology.

Keywords: Fuel Cell, Power, Multivariable, Feedback Control, Mechatronics

1 Introduction

The fuel cell (FC) principle dates back to the early 1800s (Schœnbein, 1839). Only recently, however, fuel cells became a promising alternative to internal combustion engines and thus are considered for transportation (automotive, marine and aerospace) applications and distributed power generation. Fuel cells are very efficient because they rely on electrochemistry rather than combustion. Specifically, water, electrical energy, and heat arise through the combination of hydrogen and oxygen. The major breakthroughs that brought recently FCs in the fore-front of attention include the development of low resistance membranes, highly diffusive electrodes, and reduced use of noble metal catalysts. Moreover, efficient power electronics and electric motors can now effectively utilize and distribute the electricity generated from the FC. All these advances led to many experimental demonstrations. It is the application of mechatronics concepts, however, that will allow the fuel cells to move from laboratories to streets, powering automobiles, or to our basements, heating and cooling our houses.

Our ability to precisely control the reactant flow and pressure, stack temperature, and membrane humidity is critical for the efficiency and robustness of the fuel cell stack system in real world conditions. These critical FC parameters should be controlled for a wide range of operating conditions, by a series of actuators such as relays, valves, pumps, compressor motors, expander vanes, fan motors, humidifiers and condensers. Precise control with low parasitic losses is the challenging goal of the FC auxiliary system. Moreover, estimation and real time diagnostics should be developed to augment the limited sensing in fuel cells. Finally, a snapshot into the FC industrial arena, namely, partnerships and joint ventures among automotive companies, component suppliers, and development laboratories indicates that there is a strong need for modular control architectures. In a FC vehicle, for example, there is the FC stack controller, the vehicle (ex. chassis, cooling) controllers, and the electric traction motor controller. Guidelines for the hierarchy and the coordination of all these controllers will allow their independent development and ensure a minimum level of integration.

The interactions among many thermal, chemical, electrical, and psychrometric subsystems require complicated models that are neither easy to compile nor simple to use in model-based controllers. This paper presents various FC subsystems, their models, and their integration from a controls and mechatronics perspective. The presentation starts with a containable FC design project that was undertaken within one semester by a team of undergraduates students. The FC design is described in detail so that the reader becomes familiar with the FC dimensions and parameter values. Despite its simplicity, it presents a concrete case study where design and control iterations are needed. The sections that follow the design project provide a comprehensive discussion of the FC system.

2 The FC Toy School Bus

A team of four senior undergraduate students in the Mechanical Engineering Department at the University of Michigan designed and built a toy bus powered by hydrogen that runs at constant speed around

[†] Supported by the National Science Foundation under contracts CMS−0201332 and CMS−0219623 and the Automotive Research Center (ARC) at the University of Michigan (UMICH).

a hilly route emitting only water. The road grades are modeled to look like a popular university route, namely, the Baits dormitory bus route between central and north campuses. The route is currently served every 15 minutes by buses powered with diesel fuel or natural gas. The semester-long project allowed us to understand the mechatronics and design issues of hydrogen-powered vehicles. The project and its pedagogical aspects stress cross-disciplinary involvement and combine control and design concepts for the analysis and synthesis of technologies important to our environment.

2.1 The FC Toy Bus Project Team

The team members are alphabetically Timothy D. Klaty, David S. Nay, Jean-Paul Pilette, and Sarah M. Yageman. The project sponsors and advisors are Huei Peng and Anna G. Stefanopoulou. The instructor of the capstone design course that formalized and evaluated the project is Steven J. Skerlos. Figure 1 shows three of the team members on the day of the project exhibit to the public and the jurors.

Figure 1: Tim, Sarah, and Dave (from left) putting the final touches to their FC toy bus.

2.2 The FC Toy Bus Propulsion

The design goals include a small size (less than 20x12x8 cm^3) and a light weight toy bus that can run for 3 hours on 15% road grades with 10 cm/s velocity. The total project budget was less than $ 1,500. The selection and sizing of the toy FC bus components was challenging because there are not many benchmark examples based on which we could get initial data. Moreover, linear scaling does not apply to the power, volume, and weight of fuel cell vehicles so we could not use published data from experimental full-size FC vehicles. Several constraints in commercially available fuel cell components in the desired range of size and weight narrowed the design parameter space considerably.

A FC stack of three (3) proton exchange membrane (PEM) cells with maximum power 3 W was identified from the fuel cell store (Fuel Cell Store, n.d.). It was fortunate that we could find a fuel cell at this lower power range, but we quickly realized that the FC toy bus will a very low specific power when compared to full size experimental fuel cell vehicles which have reached 200 W/kg (Friedlmeier *et al.*, 2001). The 3 W FC stack weighs 1 kg with dimensions 89x89x51 mm^3. Therefore, the FC stack will occupy a fifth of the total bus volume. Moreover, a quick calculation shows that the FC stack weight alone will be a fourth (1/4) of the total weight that the fuel cell can drive uphill a 15% grade at 10 cm/s speed assuming 20% powertrain efficiency (3 W $\approx$ 4 kg 9.81 m/s^2 0.15 0.1/ 0.2).

More technical details were requested from the fuel cell manufacturer. The nominal fuel cell stack voltage V_{st} was specified as 2.4 V at 1 Amp of current. The FC stack relies on convection for air (oxygen) feed and cooling without requiring a blower. A low pressure hydrogen feed with minimum supply of 2.2 L/hr of hydrogen was required. The specified supply corresponds to hydrogen excess ratio λ_{H_2}=(H_2 supplied)/(H_2 reacted)=1.61 based on the H_2 reacted to support 1 A of current. Specifically, electrochemistry principles are used to calculate the rate of hydrogen consumption in the fuel cell reaction based on the stack current I=1 A, the number of cells n=3, the hydrogen molar mass M_{H_2}=2.02 g/mole, the hydrogen density ρ_{H_2}=0.0827 g/l at 20 C and 100 kPa, and the Faraday number F=96485

$$H_2 \text{ reacted} = \frac{nI}{2F}\frac{M_{H_2}}{\rho_{H_2}}3600 = 1.37 \text{ l/hr}. \qquad (2.1)$$

The next step was the identification and sizing of the on-board hydrogen storage. Similarly to the fuel cell selection, the commercially available hydrogen storage options are very limited for the desired power and volume range. A metal hydride storage bottle was identified from the fuel cell store. Metal hydride tanks are alternatives to the liquefied cryogenic or compressed hydrogen storage. The metal hydride absorbs hydrogen and releases heat as the tank is filled with hydrogen. Conversely, the hydrogen is released by reducing the pressure and supplying heat (Jeong and Oh, 2002).

The metal hydride bottle was specified as absorbing and releasing 20 l of hydrogen in a volume of 0.74 l and weighs 366 g. The bottle could give us nine continuous hours of run time, based on the 3 Watt fuel cell's required supply rate of 2.2 L/hr. It was not clear at that point how we could ensure this H_2

supply rate, but the manufacturer suggested to operate the fuel cell stack without restricting the anode exit. This mode of operation is also known as "open-ended anode". The actual running time that was finally achieved by the FC toy bus was 3.6 times lower than expected indicating high hydrogen losses, or lower stored H_2 volume.

2.3 The Electric Powertrain

Having specified the fuel cell power (voltage and current) and ensured adequate hydrogen supply the powertrain can be designed as follows. The 2.4 V and 1 A is sent to the DC/DC converter where it is stepped up to an output voltage required for the traction motor. A schematic of the overall powertrain is shown in Fig. 2.

In selecting a motor, several requirements had to be outlined. These included the power that would be needed to drive the toy bus, and any additional features, such as low power consumption, integrated encoder feedback, and a small size. The power requirements was satisfied by the Micromo 1524SR DC motor with an integrated 16 line magnetic encoder. The motor achieves a range of 1.73 W maximum power output with 0.45% efficiency (requires 3.84 W input power) or 0.76 W output power with the maximum efficiency 0.76% (requires 1.0 W of input power). The DC motor operates at an input voltage range of 5-6.5 V with the optimum being equal to 6 V.

Anticipating some voltage drop from the fuel cell we chose a DC/DC converter such that the quoted FC stack voltage 2.4 V is stepped up to 6.5 V in the DC/DC output. The DC/DC converter is implemented using a LM2578A switching regulator by National Semiconductor. The output of the DC/DC converter is sent to a BASIC Stamp controller and a transistor-switching module for current control to the DC motor. The BASIC Stamp controller draws $I_{cntr} = 8$ mA at 6.5 V, and it outputs 4000 instructions per second. The encoder, drawing $I_{encd} = 8$ mA, measures the angular velocity of the motor and outputs that to the Basic Stamp. The inputs to the transistor-switching module are the DC/DC converter power output and the output of the BASIC Stamp controller. The heart of this switching module is a TO-92 type transistor made by Zetex that draws $I_{trns} = 40$ mA.

The motor intakes the current from the transistor-switching module, and uses it to mechanically rotate the shaft at a speed that depends on the current delivered. The maximum current that is delivered to the motor is

$$\begin{aligned} I_{m,in} &= I_{dc,out} - I_{loss} \\ &= \eta_{dc} P_{fc} / V_{dc,out} - (I_{cntr} + I_{trns} + I_{encd}) \\ &= 0.85\ 2.4/6.5 - 0.008 - 0.008 - 0.04 \\ &= 0.258 \text{ A}. \end{aligned} \tag{2.2}$$

The transistor-switching module can then regulate its electrical output and consequently control the motor speed up to a maximum of 6 V and 250 mA to go uphill. A current of 0.250 A corresponds to motor output of 1.113 W with 71.6% efficiency and 7700 rpm based on the manufacturer map. A 152:1 planetary gear results in an axle rotation speed of 53 rpm. The axle's rotational speed is then geared up with 3.8 cm diameter wheels which gives the toy bus a speed of 10 cm/sec around the track.

In summary, the toy FC bus has the following subsystems shown in Fig. 2: metal hydride storage bottle, 3 W fuel cell, DC/DC converter, basic stamp controller, transistor switching module, 6 V DC motor, digital encoder, planetary geartrain, wheels/chassis, steering, and track.

2.4 The Nitty-Gritty

The BASIC stamp controller processes the measured rotational speed of the motor by counting the encoder pulses within 4 ms. The controller then sends a high or low voltage signal to the transistor that in turn controls the current to the motor. A 2kΩ resistor is sized and used to match the high-low voltage from the BASIC stamp controller to the on-off voltage inputs to the transistor.

Since the motor will be, in effect, turning on and off very rapidly, there will need to be some safeguards to protect both the motor and the electronics. Due to the motor's inherent inertia, when no voltage is being applied, the motor will continue to spin and will force current through the line. This could easily short out the transistor if not accounted for. To protect against this, a fly-back diode was placed in parallel with the motor as a safety valve. Also, to eliminate voltage spikes due to the transistor switching a small capacitor (100 pF) was added in parallel.

The track was designed as a figure-eight with a bridge to cross over the lower loop. It was manufactured of plywood and plaster was used at the beginning and the end of the hills to allow for a gradual incline. A groove in the middle of the track was used to to guide the front steering mechanism of the bus, which was just a hinge that was attached to the front pivoting axle of the toy bus.

The chassis was designed and laser cut out of 0.25" thick plexiglass. Several layers were stacked and fused with methylene chloride solvent to support the weight of the fuel cell and electronics and prevent excessive bending. The fuel cell stack was placed in the front of the vehicle to allow unobstructed air flow. To accommodate the rear-wheel drive and achieve a good weight balance we placed the hydrogen tank with all the electronics and the electric drive in the rear, as shown in Fig 3. We manufactured two supports so that the bottle could slide in and out easily for refill-

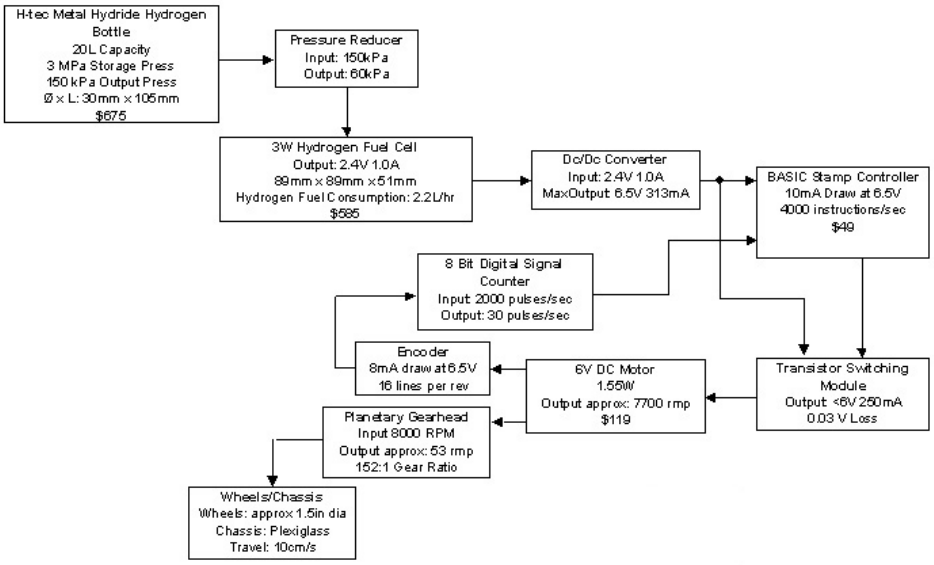

Figure 2: The information or energy flow for the powertrain components along with specifications.

ing. Finally the roof of the bus could be removed to allow for easy access to the components.

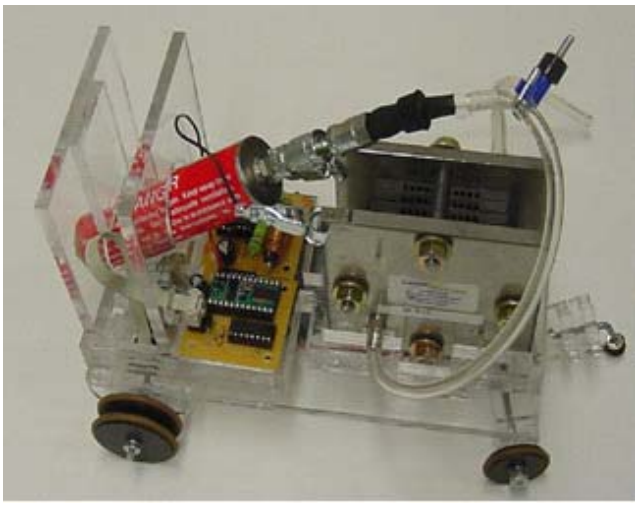

Figure 3: The components arranged in their final position in the chassis.

2.5 Hybrid FC+Battery Power

After frantic preparation and multiple checks of the individual components the students connected all the parts except the H_2 supply. We took the toy bus and its track outside the lab for fear of a potential H_2 leak. The fully charged metal hydride tank was connected to the fuel cell anode inlet and FC toy bus started spinning its wheels.

The toy bus ran through the flat part of the track but was unable to negotiate the 15% grade. Further investigation showed us that the FC voltage dropped to 1.8 V at 1 A current which could not pull the FC toy bus up the specified grade. The low voltage (0.6 V per cell) was more realistic in hindsight of other published data, so we could not really complain to the manufacturer except ask for a FC with larger active area that would allow higher current at 0.6 V per cell, or the integration of one more cell into the stack. We were, however, reluctant to request a new fuel cell stack because a new FC volume and weight would require substantial re-design.

Power augmentation with batteries was an obvious design option and offered an easy solution to the problem. Indeed, when three AA batteries were added in parallel to the output of the DC/DC converter, the FC-hybrid toy bus could climb the track slopes. The three batteries did not add any significant weight and they could fit under the hydrogen tank without any modification. The small voltage difference between the FC+DC/DC branch and the battery branch of the electric circuit allowed us to directly connect the two power sources in parallel. No special circuit was needed to guard against current flow from the battery to the fuel cell due to the slightly higher FC voltage.

The electric and power flow configuration of full size hybrid FC vehicles is very similar to our approach especially when a high voltage battery is sized and connected in parallel to the load that (i) maintains constant electric-bus voltage despite FC stack voltage variations, (ii) acts as a load buffer to the Fuel Cell stack. We describe different hybrid configurations, their benefits and drawbacks in Section 3.4.

2.6 Results and Lessons Learned

The bus could run for 2.5 continuous hours in the specified track starting with a full hydrogen tank. The batteries remain 80% full after the 2.5 hour run. Note here that the batteries alone cannot even make

Table 1: Fuel cell toy bus performance

Performance Measures	FC toy bus	NECAR4
Power density (W/m^2)	300	5000
Specific power (W/kg)	3	200
Efficiency (tank-to-wheel in mi/gal of gasoline)	3.75	60

the wheels spin on a flat terrain indicating that the FC is supplying most of the toy bus traction power.

Despite the overall project success, neither the FC stack nor the metal hydride tank met their original design specifications. Based on the 20 L (1.6 g) of H_2 stored in the metal hydride tank and the 1 km of distance travelled (10 cm/s for 2.5 hr) we found that the FC toy bus fuel consumption is equivalent to 1.6 km/l (3.75 mi/gal) of gasoline fuel. In comparison, the NECAR 4 FC experimental full size vehicle* achieves 25 km/l (60 mi/gal) of gasoline fuel as summarized in Table 1.

In an effort to identify the reasons for the low efficiency one has to understand the fuel cell system fundamental parameters, especially, the hydrogen and air flow rates, the membrane humidity, and the stack temperature. First, the FC stack we selected relies on convection for its air supply and cooling. Increasing the air flow with a fan might have improved the FC voltage at the expense of increased parasitic power to spin the fan and the additional mass and volume associated with the fan. Second, there is no humidification of the incoming air that might dry the membranes and increase the total cell resistance. External humidification is however cumbersome and excessive vapor generation causes many problems to the FC and the electronics in the proximity. Finally, the hydrogen flow discharged by the metal hydride tank depends on the tank temperature. As the tank releases hydrogen, it becomes cold, which restricts the release of further hydrogen. Considerable vapor condensation of the ambient humidity during the 2.5 hour operation is stark evidence of this cooling effect. Insulating the tank and integrating an isolated thin heating element might have improved the overall system performance.

The FC toy school bus project was accomplished as an exercise in defining and integrating the powertrain components of an electric car. The FC stack was treated as a (heavy rechargeable) battery that provided current at a nominal voltage. Upon completion of the project, it was obvious to all of us that a FC-powered powertrain is more complex and depends on optimization of the whole system instead of individual components.

*In March 1999, DaimlerChrysler introduced NECAR 4, a compact fuel-cell-powered car fuelled with liquefied hydrogen (LH_2) with approximately 450 km range (Friedlmeier *et al.*, 2001).

3 Fuel Cell Operation

Fuel cell systems (FCS) require the integration of chemical, fluid, mechanical, thermal, electrical, and electronic subsystems as highlighted by the FC toy bus project. Understanding the important physical variables and their underlying interactions is indispensable for the system design and the overall performance. In this section we present the principles of fuel cell operation with the goal to highlight the mechatronics and cross-disciplinary aspects of FCSs.

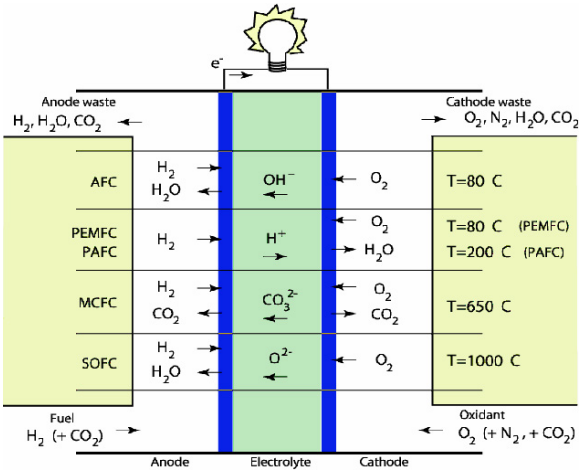

Figure 4: Fuel Cell Types

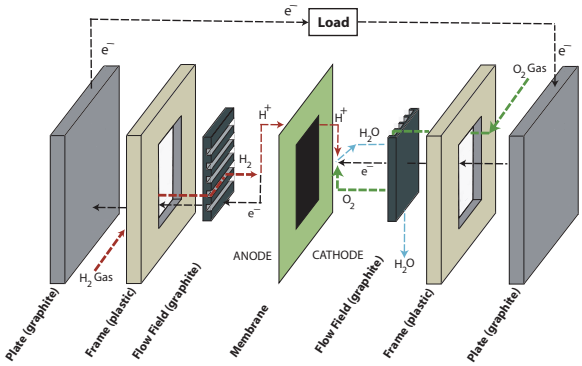

Figure 5: Fuel cell component description

There are different types of fuel cells (U.S. Department of Energy *et al.*, 2002) distinguished mainly by the type of electrolyte used in the cells, namely, polymer electrolyte fuel cell, (PEMFC, also known as proton exhange membrane fuel cells), alkaline fuel cell (AFC), phosphoric acid fuel cell (PAFC), molten

carbonate fuel cell (MCFC), and solid oxide fuel cell (SOFC) as shown in Figure 4. The differences in cell characteristics, cell material, operating temperature, and fuel, make each type of fuel cell suitable for different applications. Operating below or near the boiling temperature of water PEMFCs and AFCs rely on protons or hydroxyl ions as the major charge carriers in the electrolyte, whereas in the high-temperature fuel cells (MCFC and SOFC) carbonate ions and oxygen ions are the charge carriers. The ability of MCFC and SOFC to operate on carbonate ions and oxygen ions makes them fuel flexible. On the contrary, the PEMFC dependency on high-purity hydrogen reactant requires novel hydrogen generation and storage technologies. PEMFC have high power density, a solid electrolyte, and long life, as well as low corrosion (Larminie and Dicks, 2000). PEM fuel cells operate in the temperature range of 50 to 100 C which allows fast start-up and shut-down. Due to their benefits and advanced stage of development, we used PEMFC for the toy bus and concentrate on PEMFC in this paper.

PEMFCs utilize the chemical energy from the reaction of hydrogen and oxygen (called from now on as fuel) to produce electricity, water and heat. As shown in Figure 5, fuel travels through inlet manifolds to the flow fields. From the flow fields, gas diffuses through porous media to the membrane. The membrane, sandwiched in the middle of the cell, typically contains catalyst and microporous diffusion layers along with gaskets as a single integrated unit. One side of the membrane is referred to as the anode, the other the cathode. The anode and cathode are more generally referred to as electrodes. The catalyst layer at the anode separates hydrogen molecules into protons and electrons ($2H_2 \Rightarrow 4H^+ + 4e^-$). The membrane permits ion transfer (hydrogen protons), requiring the electrons to flow through an external circuit before recombining with protons and oxygen at the cathode to form water ($O_2 + 4H^+ + 4e^- \Rightarrow 2H_2O$). This migration of electrons produces electricity, which is the useful work. The overall reaction of the fuel cell is therefore $2H_2 + O_2 \Rightarrow 2H_2O + Heat$.

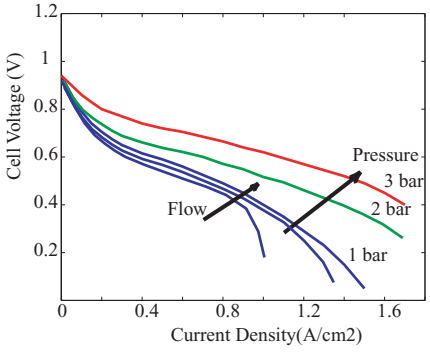

Figure 6: Polarization curves for different cathode pressures.

The electrical characteristics of fuel cells are normally given in the form of a polarization curve, shown in Figure 6, which is a plot of cell voltage versus cell current density (current per unit cell active area) at different reactant pressures and flows. Stack temperature and membrane water content also affect the fuel cell voltage. The difference between the actual voltage and the ideal voltage[†] represents the loss in the cell which turns into heat. As more current is drawn from the fuel cell, the voltage decreases, due to fuel cell electrical resistance, inefficient reactant gas transport, and low reaction rate. Lower voltage indicates lower efficiency of the fuel cell, hence low load (low current) operation is preferred. Operation at low load requires a large fuel cell stack and has detrimental consequences to the overall volume, weight, and cost.

Instead of over-sizing the FC stack, a series of actuators such as valves, pumps, blowers, expander vanes, fan motors, humidifiers and condensers shown in Fig. 7 are used to control critical FC parameters for a wide range of current, and thus, power setpoints. The auxiliary actuators are needed to make fine and fast adjustments to satisfy performance, safety and reliability standards that are independent of age and operating conditions (Yang *et al.*, 1998). The resulting multivariate design and control synthesis task, also known as balance of plant (BOP), is complex because of subsystem interactions, conflicting objectives, and lack of sensors. We summarize next the main control tasks and point to the interactions and conflicts among the main FC subsystems: (i) reactant supply system, (ii) heating and cooling system, (iii) humidification system, and (iv) power management system.

3.1 Reactant Flow Management

The reactant flow subsystem is necessary to rapidly replenish the depleted hydrogen and oxygen associated with the current drawn (load) from the anode and cathode. A low partial pressure of oxygen (hydrogen) in the cathode (anode) causes oxygen (hydrogen) starvation that damage the FC or can significantly reduce its life (Yang *et al.*, 1998). The hydrogen and air supply must be coordinated in a way that the pressure difference across the fuel cell membrane is small to avoid membrane damage. To minimize resistive losses, membranes are very thin. The desired air pressure is slightly lower than the hydrogen pressure to avoid air leaks towards the anode which can form combustible mixture. Issues associated with the hydrogen generation or storage are not discussed in this paper. Models, controllers, and references for a natural gas fuel processor can be found in (Pukrushpan *et al.*, 2004*a*). Details for hydrogen generation using aqueous Borohydride solutions are in (Amendola *et al.*, 2000). Information on hydrogen storage us-

[†]The ideal standard voltage for a fuel cell in which H_2 and O_2 react is 1.18 V when the resulting water product is in gaseous form.

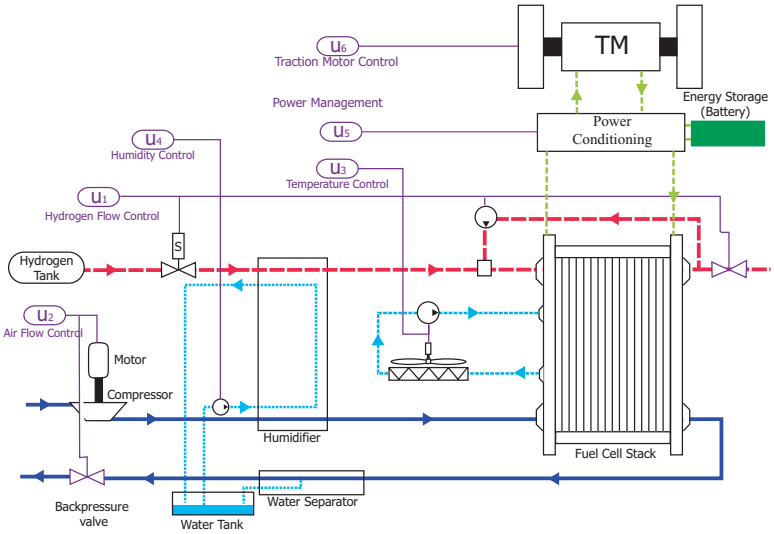

Figure 7: Fuel Cell Powertrain System

ing metal-hydride tanks can be found in (Jeong and Oh, 2002).

Passive FC systems such as the PEMFC that we used in the toy bus project, rely on convective flow with low power density. In low cost FC systems, a fixed speed (or three speed) motor, is used for the air supply to satisfy maximum traction requirements. At low flow demands the motor is a mere parasitic loss that decreases the overall propulsion efficiency at low loads, creates start-up problems and, as we shall discuss next, affects adversely the MEA hydration. To avoid these problems, a compressor (or a blower) motor control command u_2 can regulate the air flow to the cathode of the FC stack. A pressure regulator u_1 as shown in Figure 7 can easily control the anode pressure to follow the cathode pressure if compressed hydrogen is available. When reformed hydrogen is supplied by a fuel processor system (FPS), the operating FC pressure is close to atmospheric to minimize losses. The cathode flow is then controlled to follow the anode flow or pressure. The responsiveness of the reactant flow system then depends on the hydrogen supply as discussed in more detail in (Pukrushpan *et al.*, 2003). The control architecture, loop tuning, and hierarchy is thus defined based in the system operating pressure and the bandwidth of the anode and the cathode supply. Although this approach is reasonable there are cases where this hierarchy is not so obvious. Multivariable control tools can help analyze the optimum architecture as presented in (Pukrushpan *et al.*, 2003).

Independently of the implications to the control architecture the cathode operating pressure is an important and free design parameter that has attracted a lot of attention, raised heated arguments, and polarized FC developers. Low pressure FC systems rely on a blower. Their benefits and drawbacks follow. Low parasitic losses come unfortunately hand in hand with low FC power density. Inexpensive off-the-shelf blowers meer the air flow specifications but they are sometimes too bulky. Analysis of the responsiveness for each configuration indicates that the low pressure system can be approximated by a first order system. The response of the low pressure system is limited by the blower inertia, whereas, the high pressure system response is higher order and depends on the supply manifold volume (Gelfi *et al.*, 2003). Lastly, blowers do not cause high temperature rise, thus eliminating the need for inlet gas cooling before the stack. Low temperatures gas, however, cannot carry a lot of humidity which makes the inlet gas humidification and water management more sensitive than the one in high pressure FC systems that uses high-custom-made compressors. There is no definitive conclusion on the best pressure system yet, but each system has its champions. Some companies explore the flexibility of having a dual pressure system and switching between high and low pressure at different operating loads.

Once the operating pressure has been determined and the control hierarchy has been allocated among actuators and performance variables, feedforward maps (lookup-tables) can be derived from the load (current drawn) to the actuators. The immediate question that arises is the availability of sensors for feedback design. Considerations of sensor cost and ruggedness have high weight on the system configuration. Pressure sensors are cheaper and more rugged so they are preferred to the mass air flow sensors. Other questions arise from the fundamental dependency between flow and pressure (Yang *et al.*, 1998):

- "Should the control problem be posed as one of pressure regulation or one of flow tracking?" in (Boettner *et al.*, 2001*b*).
- "Should we control an additional backpressure throttle in the cathode to allow better regulation

of both flow and pressure?" in (Yang *et al.*, 1998; Rodatz *et al.*, 2003; Pischinger *et al.*, 2001).

Recent simulation results in (Pukrushpan *et al.*, 2004*b*) indicate that air flow tracking augmented with supply manifold pressure and FC stack (average cell) voltage measurements reduces oxygen starvation during load transients. The voltage measurement improves system observability and thus enables a higher gain controller in the configuration of Fig. 8. Using the stack voltage measurement as a stand-alone virtual starvation sensor might be difficult in practice because voltage depends on other variables such as hydrogen partial pressure (Arcak *et al.*, 2003) and membrane humidification (dryness and flooding) (Rodatz *et al.*, 2003). Currently, voltage is used in diagnostic and emergency shut-down procedures due to its fast reaction to oxygen starvation, but its utility and use in a feedback design has not been fully explored.

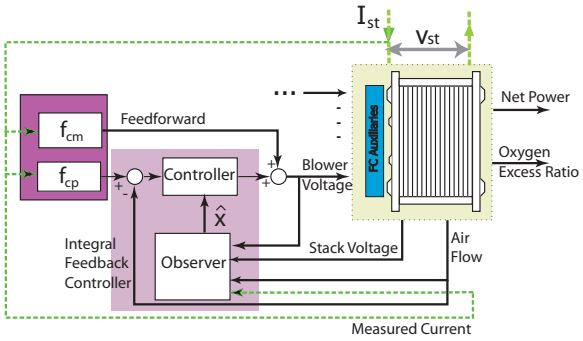

Figure 8: Potential controller architecture for the air flow management

Efforts have been devoted in controlling the reactant flow system using only voltage and current measurements and inferring power. Specifically, a single-input single-output (SISO) controller between the compressor motor voltage and the delivered current or power to the traction motor is cited in (Lorenz *et al.*, 1997). As shown in (Mufford and Strasky, 1999; Pukrushpan *et al.*, 2004*b*), the input-output system (blower to power) when no secondary energy storage elements are included is non-minimum phase, thus limiting the achievable bandwidth.

To prevent stack starvation, the stack current signal is typically filtered by a low-pass filter to allow enough time for the air supply system to increase air flow to the cathode. Since this solution slows down the fuel cell power response, it is desirable to use a current limiter based on a reference governor (Sun and Kolmanovsky, 2004) or a model predictive controller (Vahidi *et al.*, 2004).

3.2 Cooling and Heating Management

A cooling and heating subsystem is needed to dissipate the heat from the FC reactions and control the temperature of the inlet reactants before entering the stack. The power range and number of cells (only 3 W from 3 cells) of the FC toy bus did not require any active cooling. However, the heat associated with the range of power needed for a typical passenger vehicle cannot be passively dissipated by convection and radiation through the external surfaces of the FC (Larminie and Dicks, 2000). Consistent low temperature (80^c) operation, thus, requires active cooling through the reactant air and the water cooling system. The active cooling is achieved by varying the speed of the cooling fan and the recirculation pump in coordination with a by-pass valve. These three control inputs (multi-input system) are not shown in the figure above and are lumped in one control signal (u_3) for simplicity.

The goal for this control loop is fast warm-up (Boettner *et al.*, 2001*b*), with no overshoot and low auxiliary fan and pump power similar to cooling system for an internal combustion engine (Cortona *et al.*, 2000). Thermal management in FCs is more challenging than the one in internal combustion engines (ICE). Specifically, the rule of thumb for the energy balance in ICEs is: 33% for mechanical energy, 33% for energy carried by the exhaust gas, and 33% for energy carried by the cooling system. The associated distribution in FC is 40/50/10 putting stringent requirements in the cooling system. Moreover, the low temperature difference between the FC and the coolant limits the effectiveness of the heat transfer from the stack to the coolant. The typical radiator heat rejection capacity is analogous to the temperature difference between the coolant (80^o C in FCs and 120^o C for ICEs) and the ambient (32^o C) as discussed in (Fronk *et al.*, 2000). Hence to achieve good heat rejection capability, FC vehicles need large radiators.

The complexity of the thermal management problem increases when the PEMFC stack is integrated with a fuel processor for H_2 generation (Colella, 2003). The complexity arises from the internal feedback loops generated from the heat exchangers as shown in Fig. 9. Heat exchangers are placed in an effort to recover the energy of the exiting flow by heating the inlet flows. The resulting systems are also known as combined heat and power (CHP) systems and exhibit slow dynamics with initial inverse responses (Tsourapas *et al.*, 2004). CHP systems require combined control and optimization of their components to achieve high efficiency without compromising the overall system responsiveness.

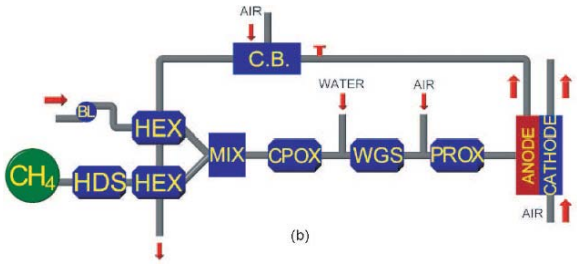

Figure 9: Schematic diagram of a combined fuel cell and a natural gas fuel processor where heat and power generation are combined for high efficiency.

3.3 Water and Humidity Management

The ability of the membrane to conduct protons is fundamental to the PEMFC operation. This ability is linearly dependent upon its water content (Zawodzinski *et al.*, 1993). On one hand, as membrane water content decreases, ionic conductivity decreases (Springer *et al.*, 1991), resulting in a decreased cell electrical efficiency, observed by a decrease in the cell voltage. This decrease in efficiency causes increased heat production which evaporates more water, in turn lowering membrane water content even more. The interaction between high temperature and low humidity creates a positive feedback loop. On the other hand, excessive water stored in the electrodes obstructs fuel flow, resulting in cell flooding (Zawodzinski *et al.*, 1993). In both cases, managing the water concentration in the electrodes is very important for increasing optimal fuel cell efficiency and extending the FC life.

A water injection or an evaporation mechanism, shown with the command u_4, is used to control the humidity of the reactants and eventually the membrane hydration. Although, passive (internal) humidification concepts are rigorously pursued (Bernardi, 1990; Watanabe *et al.*, 1996), external active control allows wider range of operation typically met in automotive applications (Yang *et al.*, 1998). As current is drawn from the FC, water is generated in the cathode and water molecules are dragged from the anode to the cathode. This transfer of vapor is known as electroosmotic drag. Additionally, the vapor concentration gradient causes diffusion of water through the membrane and is referred to as back diffusion. The magnitude and direction of the net vapor flow through the membrane (anode to cathode or cathode to anode) is a function of the relative magnitudes of these two transport mechanisms.

Hence, perturbation in the FC humidity can be caused by different mechanisms as characterized in (McKay and Stefanopoulou, 2004): (i) the water generated during the load increase(current drawn from the FC), (ii) changes in absolute and relative reactant pressure across the membrane, (iii) changes in the air flow out of the fuel cell that carries vapor, and dries the membrane, and (iv) changes of the FC temperature, and thus, the saturation pressure. These mechanisms indicate strong and nonlinear interactions among the humidity control task, the reactant flow management loop, the heat management loop and the power management loop. The interactions are so strong that part of the hydrogen flow subsystem is dedicated to the water management in the anode. The anode is particularly vulnerable to flooding since it is dead-ended so it is prone in accumulating vapor and inert gas. Various ingenious mechatronic solutions have been proposed to abate anode flooding (Rodatz *et al.*, 2002). These investigations aim to optimize the inefficient practice of purging or recirculating the anode contents utilizing a downstream anode valve and a pump as shown in Fig. 7.

Pointing to the complexity of the humidification task the authors in (Büchi and Srinivasan, 1997) note that the humidification components account for 20% of stack volume and weight. The stack, on the other hand, under-performs with 20%-40% lower voltage if there is no proper humidication control.

3.4 Power Management

The simplest power configuration comprises of a FC, DC/DC converter, and a traction motor (TM) (DC motor or inverter+AC motor). The DC/DC converter can make the FC voltage output compatible with the input to the inverter or the dc motor (Wang *et al.*, 1998; Larminie and Dicks, 2000; U.S. Department of Energy *et al.*, 2002). Typically, the traction motor is viewed as a load from the FC+DC/DC side. In the worst case scenario, the load can be modeled as an instantaneous resistive load (R in Fig. 10). The DC/DC converter must then maintain constant output voltage V_{out} (electric bus) during this fast load change. The voltage regulation can be achieved by adjusting the duty ratio d of the DC/DC converter pulsewidth. The fuel cell stack can be modeled with its equivalent impedance Z_{FCS}. Note here that we need to consider the closed loop FC system impedance, i.e., calculate the FC impedance once the air flow, the thermal, and the humidification controllers are designed (Pukrushpan *et al.*, 2004*b*).

The DC/DC converter switching frequency, capacitor, and inductor are sized so that the converter produces acceptable ripples in the output voltage and fuel cell current. The low-voltage/high-current output characteristics make the overall switching and nonlinear FC+DC/DC system very sensitive to load variations (Appleby and Foulkes, 1989). The averaged and linearized system exhibits non-minimum phase dynamics from d to V_{out}, and thus, the DC/DC feedback loop has bandwidth limitations (Krein, 1998). To better appreciate the difficulties consider V_{in}= 250 V, I_{in} = 200 A for a 50kW nominal FC power. If the motor's nominal voltage is V_{out}=400 V,

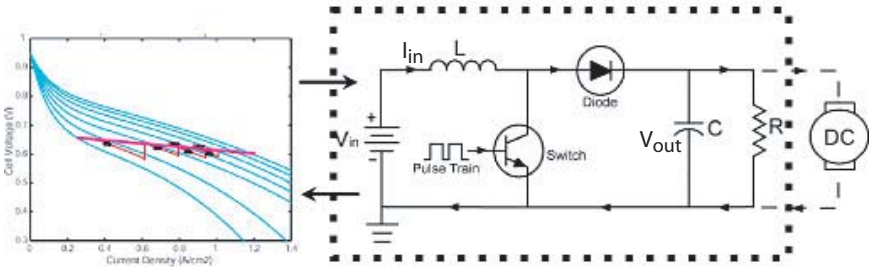

Figure 10: Simplified electric circuit for a FC connected to a traction motor through a DC/DC converter.

the DC/DC converter switching frequency is 50kHz, and the ripple limit is chosen to be less than 1%, then the open loop plant (from d to V_{out}) has an ORHP zero at 2009 rad/s. So there is a big undershoot (nearly 50 V) when we step up the duty cycle from 37.5% to 50%. A PI controller shows that the transient time has to increase from 2 ms to 100 ms, if the undershoot has to decrease from 50 V to 2 V.

Hybrid power management studies include secondary large batteries (Akella *et al.*, 2001; Boettner *et al.*, 2001*a*) and/or ultracapacitors (Rodatz *et al.*, 2004). There are several electrical configurations that have been considered for hybrid (FC and battery) systems. An excellent discussion for these issues is given in (U.S. Department of Energy *et al.*, 2002; Rajashekara and Martin, 1995). The DC/DC converter control problem gets simplified when a high voltage battery is connected in parallel between the DC/DC converter and the load. The battery supports the main electric bus voltage, and the duty ratio of the DC/DC converter controls the current drawn from the fuel cell. Noncausal (also known as "backwards-looking") optimization methods can then be used to evaluate energy storage and regenerative braking strategies.

4 Time Constants

Fuel cells are considered for many different applications with emphasis to commercial power generation and automotive applications. The challenges in automotive applications arise partly due to the low cost requirements and partly due to their high bandwidth requirements. Drivers, for example, are perceptive to lags longer than 0.2 s during acceleration requests. The relevant time constants for an automotive propulsion-sized PEMFC stack system are:

- Electrochemistry $O(10^{-19})$ sec
- Hydrogen & air manifolds $O(10^{-1})$ sec
- Membrane water content $O(10^{0})$ sec for the cathode and $O(10^{1})$ sec for the anode
- Flow control/supercharging devices $O(10^{0})$ sec
- Vehicle inertia dynamics $O(10^{1})$ sec
- Cell and stack temperature $O(10^{2})$ sec

where O denotes the order of magnitude. The fast transient phenomena of electrochemical reactions have minimal effects in automobile performance and can be ignored. The relatively slow dynamics of the vehicle inertia and the cell and stack temperature may be lumped in a separate system which is equipped with a separate controller. The vehicle velocity and stack temperature can then be considered as constant or slow varying parameter for other faster subsystems. A linearization of the gas humidity model in (McKay and Stefanopoulou, 2004) revealed that the eigenvalues associated with the cathode and the anode humidity depend on the cathode and anode outlet gas flow, respectively. This finding substantiates the general belief that the humidity dynamics cannot be easily decoupled from the temperature and flow dynamics. Indeed, the air exiting the stack carries considerable vapor and affects the FC humidification. Moreover, the air flow dynamics correspond to time constants that are easily perceived by the driver. Hence, the air flow dynamics described by the manifold filling and supercharging devices need to be considered carefully in the control system design.

5 Experimental Set up

One of the most challenging characteristic in fuel cells is its spatially varying behavior depending on the local temperature and the gas composition at the membrane surface. Due to the complexity inherent with distributed parameter analysis, the geometric complexity of the stack design, as well as the difficulty associated with taking measurements at the membrane surface or within the electrodes of large multicell stacks (Mench *et al.*, 2003), we use lumped parameter models calibrated with experimental data. Unfortunately, experimental data necessary for understanding, predicting, and controlling the unique transient behavior of PEMFC stacks are not easy to obtain. It is not easy for example to obtain data from industry or laboratories due to the confidential and competitive nature of the information. Also commercial FC units are typically bundled with closed architecture controllers that obstruct system identification techniques.

To address the need for transient data and experi-

mental validation of models and controllers a laboratory was established with partial funding from the National Science Foundation (CMS-0219623). A 24-cell, 300 cm^2, 1.4kW PEMFC stack was purchased from the Schatz Energy Research Center (SERC) at Humboldt State University and installed at the Fuel Cell Control Laboratory (FCCL) at the University of Michigan. Figure 11 displays the instrumented stack installed on the test station at the University of Michigan's Fuel Cell Control Laboratory. Protruding from the stack endplates are the relative humidity, temperature and pressure transducers as well as gas and coolant connections. Arrows are used to show the flow of hydrogen and air into and out of the stack.

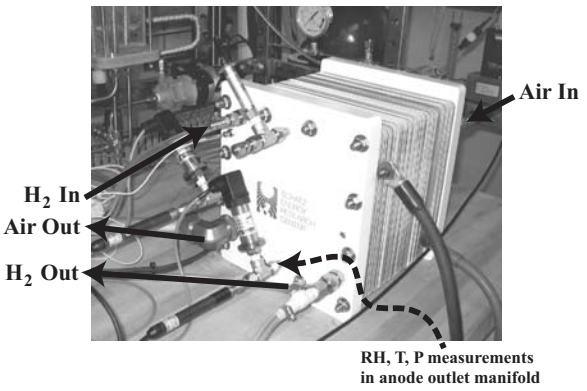

Figure 11: Instrumented SERC fuel cell stack

The experimental set-up allows the design, testing, and integration of real-time time software for simulation, optimization, control, and diagnostics in transient load conditions. The laboratory is equipped with data acquisition from LabView, hardware and software safety system, oil-less air compressor for precise air flow control, di-ionized water system, and controllable cooling system through heat exchangers.

6 Conclusions

This paper presents the challenges of sizing and controlling fuel cell systems. We also point to recent papers in the FC literature with control and mechatronics results. There have been many publications that express the need for systematic control approach for fuel cell power plans. Most of these publications are in the Chemistry and Chemical Engineering literature so the opportunities are not easily accessible from the control community. The field is fast evolving and there is a lot of excitement but also a lot of challenges. Physics-based models and model-based control design can provide the systematic tools for addressing these challenges. Finally, fuel cells provide exciting test beds for educational activities. They require multidisciplinary teams and are very rewarding due to their environmental importance.

Acknowledgment

Many thanks go to J. Luntz (UMICH) for his help and advice on the power electronics and controller implementation for the FC toy bus and also to H. Peng (UMICH), J. Sun (UMICH), P. Lehman (SERC), C. Chamberlin (SERC), L. Guzzella (ETH), and Y.G. Guezennec (OSU) for all the helpful discussions. I also thank the FC toy bus team and my students Jay Pukrushpan, Denise McKay, Ardalan Vahidi, Kyung-Won Suh, Vasilis Tsourapas, and Vera Simms.

References

Akella, S., N. Sivashankar and S. Gopalswamy (2001). Model-based systems analysis of a hybrid fuel cell vehicle configuration. *Proceedings of 2001 American Control Conference* **3**, 1777–1782.

Amendola, S.C., S.L. Sharp-Goldman, M.S. Janjua, N.C. Spencer, M.T. Kelly, P.J. Petillo and M. Binder (2000). A safe, portable, hydrogen gas generator using aqueous borohydride solution and ru catalyst. *International Journal of Hydrogen Energy* **25**, 969–75.

Appleby, A.J. and F.R. Foulkes (1989). *Fuel Cell Handbook*. Van Nostrand Reinhold. New York.

Arcak, M., H. Gorgun, L.M. Pedersen and S. Varigonda (2003). An adaptive observer design for fuel cell hydrogen estimation. *Proceedings of the 2003 American Control Conference* pp. 2037–2042.

Bernardi, D.M. (1990). Water-balance calculations for solid-polymer-electrolyte fuel cells. *Journal of Electrochemical Society* **137**(11), 3344–3350.

Boettner, D.D., G. Paganelli, Y.G. Guezennec, G. Rizzoni and M.J. Moran (2001*a*). Component power sizing and limits of operation for proton exchange membrane (PEM) fuel cell/battery hybrid automotive applications. *Proceedings of 2001 ASME International Mechanical Engineering Congress and Exposition*.

Boettner, D.D., G. Paganelli, Y.G. Guezennec, G. Rizzoni and M.J. Moran (2001*b*). Proton exchange membrane (PEM) fuel cell system model for automotive vehicle simulation and control. *Proceedings of 2001 ASME International Mechanical Engineering Congress and Exposition*.

Büchi, F.N. and S. Srinivasan (1997). Operating proton exchange membrane fuel cells without external humidification of the reactant gases. *Journal of Electrochemical Society* **144**(8), 2767–2772.

Colella, W. G. (2003). Design considerations for effective control of an afterburner sub-systemin a combined heat and power (chp) fuel cell system (fcs). *Journal of Power Sources*.

Cortona, E., C. Onder and L. Guzzella (2000). Model-based temperature control for improved fuel economy of si-engines. *Proceedings of the 3rd IFAC Workshop on Advances in Automotive Control*.

Friedlmeier, G., J. Friedrich and F. Panik (2001). Test experiences with the daimlerchrysler fuel cell electric vehicle NECAR 4. *Fuel Cells* **1**, 92–96.

Fronk, M.H., D.L. Wetter, D.A. Masten and A. Bosco (2000). PEM fuel cell system solutions for transportation. *SAE Paper 2000-01-0373*.

Fuel Cell Store (n.d.). Products. http://www.fuelcellstore.com.

Gelfi, S., A.G. Stefanopoulou, J. Pukrushpan and H. Peng (2003). Dynamics and control of low and high pressure fuel cells. *Proceedings of the 2003 American Control Conference* pp. 2049–2054.

Jeong, K. S. and B. S. Oh (2002). Fuel economy and life-cycle cost analysis of a fuel cell hybrid vehicle. *Journal of Power Sources* **105**, 58–65.

Krein, P. T. (1998). *Elements of Power Electronics*. Oxford University Press.

Larminie, James and Andrew Dicks (2000). *Fuel Cell Systems Explained*. John Wiley & Sons Inc. West Sussex, England.

Lorenz, H., K-E Noreikat, T. Klaiber, W. Fleck, J. Sonntag, G. Hornburg and A. Gaulhofer (1997). Method and device for vehicle fuel cell dynamic power control. *United States Patents 5,646,852*.

McKay, D. A. and A. G. Stefanopoulou (2004). Parameterization and validation of a lumped parameter diffusion model for fuel cell stack membrane humidity estimation. *IEEE Proceedings of 2004 American Control Conference*.

Mench, M. M., Q. L. Dong and C. Y. Wang. (2003). In situ water distribution measurements in a polymer electrolyte fuel cell. *Journal of Power Sources*.

Mufford, W.E. and D.G. Strasky (1999). Power control system for a fuel cell powered vehicle. *United States Patents 5,991,670*.

Pischinger, S., C. Schönfelder, W. Bornscheuer, H. Kindl and A. Wiartalla (2001). Integrated air supply and humidification concepts for fuel cell systems. *SAE Paper 2001-01-0233*.

Pukrushpan, J.T., A.G. Stefanopoulou and H. Peng (2004*a*). *Control of Fuel Cell Power Systems: Principles, Modeling, Analysis, and Feedback Design*. Springer Verlag.

Pukrushpan, J.T., A.G. Stefanopoulou and H. Peng (2004*b*). Controlling fuel cell breathing. *IEEE Control Systems Magazine*.

Pukrushpan, J.T., A.G. Stefanopoulou, S. Varigonda, L.M. Pedersen, S. Ghosh and H. Peng (2003). Control of natural gas catalytic partial oxidation for hydrogen generation in fuel cell applications. *Proceedings of the 2003 American Control Conference* pp. 2030–2036.

Rajashekara, K. and R. Martin (1995). Electric vehicle propulsion systems present and future trends. *Journal of Circuits, Systems and Computers* **5**(1), 109–129.

Rodatz, P., G. Paganelli, A. Sciarretta and L. Guzzella (2004). Optimal power management of an experimental fuel cell/supercapacitor-powered hybrid vehicle. *to appear in Control Engineering Practice*.

Rodatz, P., G. Paganelli and L. Guzzella (2003). Optimization of fuel cell systems through variable pressure control. *Proceedings of the 2003 American Control Conference* pp. 2043–2047.

Rodatz, Paul, Akinori Tsukada, Michael Mladek and Lino Guzzella (2002). Efficiency improvements by pulsed hydrogen supply in PEM fuel cell systems. *Proceedings of the 15th IFAC Triennial World Congress*.

Schœnbein, C.F. (1839). The voltaic polarization of certain solid and fluid substances. *Philosophical Magazine* **14**, 43–45.

Springer, T.E., T.A. Zawodzinski and S. Gottesfeld (1991). Polymer electrolyte fuel cell model. *Journal of Electrochemical Society* **138**(8), 2334–2342.

Sun, Jing and Ilya Kolmanovsky (2004). A robust load governor for fuel cell oxygen starvation protection. *Proceedings of 2004 American Control Conference*.

Tsourapas, V., J. Sun and A.G. Stefanopoulou (2004). Modeling and dynamics of a fuel cell combined heat power system for marine applications. *in Proceedings of 8th WSEAS International Conference on Systems*.

U.S. Department of Energy, Office of Fossil Energy and National Energy Technology Laboratory (2002). *Fuel Cell Handbook*. EG&G Technical Services, Inc, Science Application International Corporation.

Vahidi, A., A.G. Stefanopoulou and H. Peng (2004). Model predictive control for power management of a hybrid fuel cell system. *IEEE Proceedings of 2004 American Control Conference*.

Wang, K., C.Y. Lin, L. Zhu, D. Qu, F.C. Lee and J.S. Lai (1998). Bi-directional DC to DC converters for fuel cell systems. *IEEE Power Electronics in Transportation* pp. 47–51.

Watanabe, M., H. Uchida, Y. Seki, M. Emon and P. Stonehart (1996). Self hymidifying polymer electrolyte membranes for fuel cells. *Journal of the Electrochemical Society* **143**(12), 3847–3852.

Yang, W-C, B. Bates, N. Fletcher and R. Pow (1998). Control challenges and methodologies in fuel cell vehicle development. *SAE Paper 98C054*.

Zawodzinski, T., C. Derouin, S. Radzinski, R. Sherman, V. Smith, T. Springer and S. Gottesfeld (1993). Water uptake by and transport through nafion 117 membranes. *Journal of the Electrochemical Society*.